Vibrational Excitation Induces Double Reaction

Kai Huang, Lydie Leung, Tingbin Lim,† Zhanyu Ning, and John C. Polanyi*

Lash Miller Chemical Laboratories, Department of Chemistry and Institute of Optical Sciences, University of Toronto, 80 St. George Street, Toronto, Ontario M5S SH6, Canada. †Present address: University College London, London Centre for Nanotechnology, 17-19 Gordon Street, London WC1H 0AH, U.K.

ABSTRACT Electron-induced reaction at metal surfaces is currently the subject of extensive study. Here, we broaden the range of experimentation to a comparison of vibrational excitation with electronic excitation, for reaction of the same molecule at the same clean metal surface. In a previous study of electron-induced reaction by scanning tunneling microscopy (STM), we examined the dynamics of the concurrent breaking of the two C—I bonds of *ortho*-diiodobenzene physisorbed on Cu(110). The energy of the incident electron was near the electronic excitation threshold of $E_0 = 1.0$ eV required to induce this single-electron process. STM has been employed in the present work to study the reaction dynamics at the substantially lower incident electron energies of 0.3 eV, well below the electronic excitation threshold. The observed increase in reaction rate with current was found to be fourth-order, indicative of multistep reagent vibrational excitation, in contrast to the first-order rate dependence found earlier for electronic excitation. The change in mode of excitation was accompanied by altered reaction dynamics, evidenced by a different pattern of binding of the chemisorbed products to the copper surface. We have modeled these altered reaction dynamics by exciting normal modes of vibration that distort the C—I bonds of the physisorbed reagent. Using the same *ab initio* ground potential-energy surface as in the prior work on electronic excitation, but with only vibrational excitation of the physisorbed reagent in the asymmetric stretch mode of C—I bonds, we obtained the observed alteration in reaction dynamics.

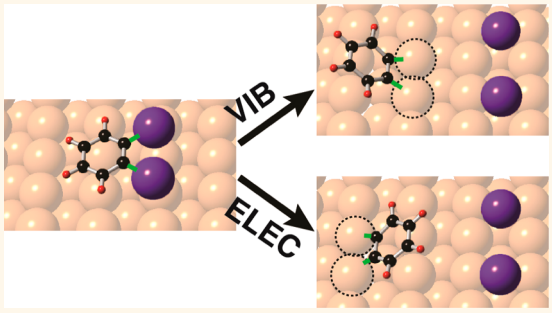

KEYWORDS: *ab initio* computations · molecular dynamics · scanning tunneling microscopy · vibrational excitation · electronic excitation · surface science · single-molecule reaction

Electron-induced reactions at a solid surface can be followed "a molecule at a time" using the tip of a scanning tunneling microscope (STM) as a source of electrons and thereafter examining the products by STM.[1−18] When a large number of electrons traverse an adsorbate, inelastic collisions can transfer energy. This causes nuclear motions that in some cases lead to surface reaction. Depending on the energy of the electrons, excitation may be *electronic* or *vibrational*. Electronic excitation occurs primarily when the electron is in the electronvolt range.[1−6,9−11,15,16,18] However, when the electron energy is low—hundreds of meV—adsorbate vibration can be excited on the ground potential surface.[12−14]

In spite of the rich literature on reactions induced by electrons from an STM tip,[1−3,5,6,9−16] comparative studies of these two different excitation mechanisms for a single system are few.[19,20] Shen *et al.*[19] were the first to compare the two mechanisms, studying electron-induced desorption of hydrogen atoms from a hydrogen-passivated Si(100) surface, induced by electrons from an STM tip. Subsequently,[21] questions have been raised in regard to the role of vibrational excitation in this reaction. More recently, Shi, Kawai, and co-workers[20] succeeded in dissociating single water molecules *via* both electronic and vibrational mechanisms on a thin MgO film supported on Ag(100). The reaction products were found to differ for the two mechanisms, yielding atomic oxygen from electronic excitation and hydroxyl from vibrational excitation. To our knowledge, the present work is the first to compare the vibrational and electronic mechanisms for a single reaction at a clean metal surface.

Here, we report the reaction dynamics of *ortho*-diiodobenzene (*ortho*-DIB) on Cu(110) by multiple excitations due to tunneling electrons in the low-energy range

* Address correspondence to jpolanyi@chem.utoronto.ca.

Received for review September 18, 2014 and accepted December 9, 2014.

Published online December 09, 2014
10.1021/nn5053074

(0.3 eV) for *vibrational* excitation and compare the results to earlier work from this laboratory for the same system employing single high-energy electrons (~1 eV) *via electronic* excitation.[22] The breaking of two C—I bonds of a single *ortho*-DIB, termed "double reaction", was found to predominate in both vibrational and electronic reactions. Three cases of two-bond breaking in the course of a reactive event have been reported recently.[15,22,23] The first involved the single-electron breaking of two adjacent bonds by charge delocalization,[22] the second single-electron breaking of a series of bonds in a molecular chain,[15] and the third single-electron breaking of two adjacent bonds, one promptly by electron attachment and the other after 0.5 ps by product vibrational excitation.[23] However, the observed product geometry differed in the case of reagent vibrational excitation from the previous case of reagent electronic excitation, giving evidence of altered binding of the chemisorbed product to the copper surface. Specifically, both the binding site and the alignment of the chemisorbed phenylene product formed by vibrational excitation of the physisorbed reagent differed significantly from that formed by electronic excitation of the reagent.

We have modeled the vibration-induced reaction employing *ab initio* molecular dynamics (MD) simulation by exciting selected normal modes of vibration in the physisorbed reagent. Of the four normal modes that represent the distortion of C—I bonds, involving stretch and bend, the asymmetric C—I stretch is shown to be the only mode capable of reproducing the binding pattern of products observed. In this computation, we used the same *ab initio* ground potential surface as in our previous work.[22] This calculation compares the dynamics of surface reaction induced by electronic excitation with that by vibrational excitation.

RESULTS AND DISCUSSION

In Figure 1, we contrast the reaction of *ortho*-DIB on Cu(110) induced by single electronic excitation of ~1 eV (at left) with that from multiple vibrational excitations employing incident electrons of 0.3 eV (at right). As established in our early work by STM and *ab initio* theory,[22] the physisorbed *ortho*-DIB molecule on Cu(110) adopts a nearly flat configuration, with the benzene ring centered at the short-bridge site and the two I atoms at short-bridge sites of the adjacent Cu row. This physisorbed geometry leads to an approximately triangular-shaped feature for physisorbed *ortho*-DIB in the STM images, as shown in Figure 1A.

Upon a voltage pulse from the STM tip, the *ortho*-DIB in Figure 1A reacted to break both C—I bonds and produced two chemisorbed I atoms and a chemisorbed phenylene (Ph′). Figure 1B,C shows the major reactive outcomes for reagent excitation by electrons of 1 eV, giving rise to reagent electronic excitation (67% out of a total of 321 cases) and electrons of 0.3 eV,

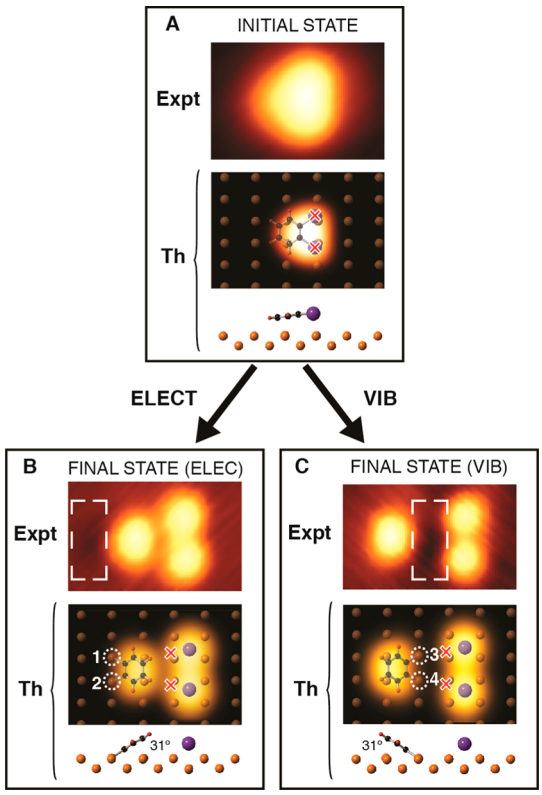

Figure 1. (A) "Expt" shows an STM image for physisorbed *ortho*-diiodobenzene on Cu(110) obtained in the present work. "Th" (theory) gives the result of *ab initio* calculation of the physisorbed geometry (top and side views), the top view being superimposed on a simulated STM image computed by bSKAN. Here, as in all subsequent panels, the red crosses indicate the position of the I atoms in the initial state. The arrow at the left below panel A ("ELECT") points to panel B ("Expt"), giving an example of the major experimental outcome of electron-induced reaction for what was shown to be single-electron excitation of physisorbed *ortho*-DIB at 1.0 eV electron energy, taken from prior work of this laboratory.[22] (B) "Th" gives the chemisorbed product geometries, viewed from top and side, and their bSKAN simulated STM image. The arrow at the right below panel A ("VIB") points to panel C, giving (for comparison with panel B) an experimental image ("Expt") of the major chemisorbed reaction products obtained in the present work as a result of excitation by multiple electrons of 0.3 eV, *i.e.*, due to vibrational excitation of the physisorbed *ortho*-DIB. (C) "Th" gives the chemisorbed product geometries, viewed from top and side, and their bSKAN simulated STM image, resulting from vibration-induced reaction. The white rectangles in B and C, Expt, indicate dark patches corresponding to the points of attachment of the phenylene to the surface. All experimental STM images in panels A—C are in 23 Å × 13 Å in size, taken at a sample bias of +0.3 V and a tunneling current of 0.2 nA.

giving reagent vibrational excitation (64% out of a total of 61 cases). The I atoms in each case occupied the nearest four-fold hollow site along the prior C—I direction in the physisorbed *ortho*-DIB. However, the phenylene fragments, Ph′, can be seen to have different binding sites (bound to Cu #1 and #2 from reagent electronic excitation and to Cu #3 and #4 from reagent vibrational excitation) and different alignment with respect to the I atom pair (bound away from the I atom side from reagent electronic excitation and bound

toward the I atom side from reagent vibrational excitation). As reported in ref 22 from STM imaging and simulations, the brightness of Ph′ in the STM images originates from its aromatic ring, whereas the adjacent dark patches correspond to the positions where Ph′ binds to the surface (white rectangles in Figure 1B,C). In the following experimental and theoretical discussion, we shall denote the two final product states as ELEC and VIB. The remaining cases for both the electronic and vibrational excitations are presented in footnote 24.

Central to the current work is the dissociation of *ortho*-DIB on Cu(110) caused by electrons of only 0.3 eV. The electronic excitation mechanism[22] can be excluded for this electron energy which falls well below the computed lowest unoccupied molecular orbital that lies at 1.0 eV above the Fermi level. This alteration in excitation mode is also reflected in the measured electron efficiency (yield) which ranged from 4.6×10^{-16} at 94 nA to 1.5×10^{-15} at 136 nA, reactive events/electron; this is 6 to 7 orders of magnitude lower than the yield of $\sim 10^{-9}$ reported in our early work employing electronic excitation.[22] In the earlier work, the excitation was attributed to a low-lying anionic state evident in the computed projected density of states. Electronic excitation is not occurring in the present case because there is no state within 0.3 eV of the Fermi level.[22] Evidence that this mechanism is vibrationally induced is given by the comparable efficiency of reaction by voltage pulses of 0.3 V in both polarities.[25,26] Vibrational excitation appears to be the most probable mechanism.

To test this excitation mechanism, we measured the reaction order, n, at a sample bias of +0.3 V, by varying the tunneling current, I. The time required for reaction of a physisorbed *ortho*-DIB under each voltage pulse was determined from a clear discontinuity in our current *versus* time spectra. The individual times required for reaction were then binned and fitted to an exponential decay function, which yielded the characteristic lifetime, τ, of the *ortho*-DIB molecule. The reciprocal of τ was the rate of reaction, R, which was then plotted against I using a log scale, as in Figure 2. The reaction order of $n = 4.4 \pm 1.2$ taken from the slope of this plot in a least-squares fit indicates that reaction occurred as a consequence of excitation by four successive electrons. In our experiments, the average time delay was estimated as 1−2 ps for successive electrons to arrive at *ortho*-DIB. Despite this delay, the molecules can suffer sequential excitation, leading to C−I bond breaking, as the vibrational lifetimes of molecules on metal surfaces are in the range of picoseconds.[27] In contrast, the lifetimes of ionic species at metal surfaces are in the range of a few femtoseconds,[28] precluding sequential excitation. It would seem most likely that the observed reaction was induced by four successive electrons of 0.3 eV, taking place by way of multiple

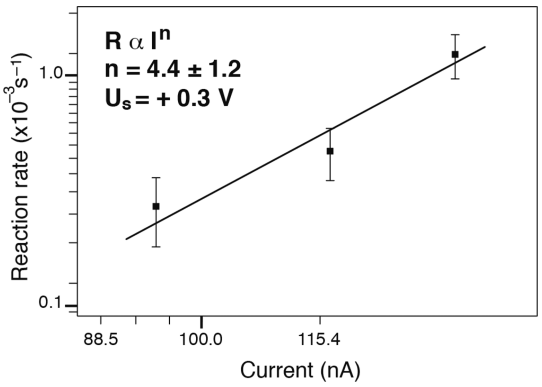

Figure 2. Reaction order of the dissociation of *ortho*-DIB on Cu(110) measured at a sample bias of +0.3 V. The reaction rate (R) is plotted as a function of current (I) using a log scale, where the slope (n) from the least-squares fit is the reaction order, determined as $n = 4.4 \pm 1.2$. Error bars are from the errors of the exponential fit of the characteristic lifetimes.

excitation of the physisorbed adsorbate to excited vibrational levels on the ground potential-energy surface. The effect of the electric field can be excluded as the primary reaction mechanism on the basis of the observed fourth-order dependence of reaction rate on current and the comparable efficiency of reaction by voltage pulses of 0.3 V in both polarities.

To further characterize the initial physisorbed state and final states (ELEC and VIB), we calculated their geometries using *ab initio* theory and simulated images for each state. As shown in Figure 1, there is satisfactory agreement between experiment and simulation. The reaction exothermicities were computed to be 2.83 eV to form final state ELEC and 2.76 eV to form final state VIB, showing similar thermodynamic stability for the two final states.[29] The computed reaction barriers to these two final states (using a nudged elastic band)[30] are also similar, both being 0.14 eV. These barriers are further reduced to 0.10 eV if one corrects for the effect of quantum zero-point energies of both initial and transition states. Such a low barrier is consistent with expectation for highly exothermic reactions.

The total available reagent excitation energy from four electrons, each at 0.3 eV, far exceeds the reaction barrier of 0.10 eV on the minimum-energy path. The vibration-induced reactive trajectories must deviate from the minimum-energy path, giving the observed pattern of reaction products. A full characterization of the reaction dynamics, including vibration-to-vibration transfer in the field of the surface, is beyond the scope of this paper. Instead, we have performed classical trajectory studies across the previously employed *ab initio* ground potential-energy surface[22] by exciting single reagent vibrational normal modes.

We compared the fundamental vibrational excitation energies computed for the physisorbed *ortho*-DIB molecule, with the values for the gaseous molecule. In the harmonic oscillator approximation, we calculated,

for *ortho*-DIB adsorbed on Cu(110), the fundamental vibrational energies as 24.4 meV for asymmetric stretch mode, 37.4 meV for the symmetric stretch mode, 38.3 meV for the bending mode parallel to the surface, and 27.7 meV for the bending mode perpendicular to the surface. The values from the gas-phase data are only available for the stretch modes, as 25.5 meV for symmetric stretch and 39.3 meV for asymmetric stretch.[31] The close resemblance of vibration in the gaseous and adsorbed *ortho*-DIB is consistent with the fact that only a small distortion occurs on physisorption.

As we are dealing with a C—I bond-breaking reaction in our dynamical studies of single-mode-induced reaction, we focus on normal modes of vibration that involve marked distortion of the C—I bonds. Four such normal modes leading to two-bond breaking are shown in Figure 3 in which panels A/B are the asymmetric/symmetric stretch mode of the C—I bond and C/D are the bending mode parallel/perpendicular to the substrate surface.[32] The physisorbed state prior to reaction is that observed experimentally and, hence, is the same in all four cases, whereas the chemisorbed final states differ from the four vibrational modes of differing symmetry.

Figure 3 provides, for four cases of the surface reaction of vibrationally excited *ortho*-diiodobenzene, a link between reagent excitation on a single potential-energy surface and the computed geometry of the chemisorbed products. This sensitivity of the dynamics to the reagent excitation is due to the existence of different paths through configuration space, leading from reagents to products.

None of the patterns of chemisorbed products shown in Figure 3 fully matched the observed product pattern from vibrational excitation in these experiments, but the asymmetric stretch mode gave the correct binding for the I atom products. We therefore performed further trajectory calculations of this mode at higher vibrational energy up to 1.2 eV, with this upper limit being set by the total energy of the four electrons of 0.3 eV.

Figure 4 gives the reactive outcomes from trajectories employing the asymmetric stretch mode at $\nu = 28$, 32, 36, and 40. We are able to reproduce the correct product pattern by vibrational excitation (see Figure 4C) at $\nu = 36$ of the asymmetric stretch mode.[33] In Figure 5, we present a series of snapshots to show the dynamics at successive times, for $\nu = 36$ excitation of the physisorbed reagent asymmetric stretch mode. Panels B and C of the dynamics computation show the aromatic ring first rotating to vertical as the new dangling bonds of the phenylene bind to the underlying copper; thereafter, in panels D and E, the ring rotates back to the horizontal as the π-orbitals of the aromatic ring engage with the surface.

Though the electron efficiency of the observed reaction is only 10^{-15} to 10^{-16} reactive events per

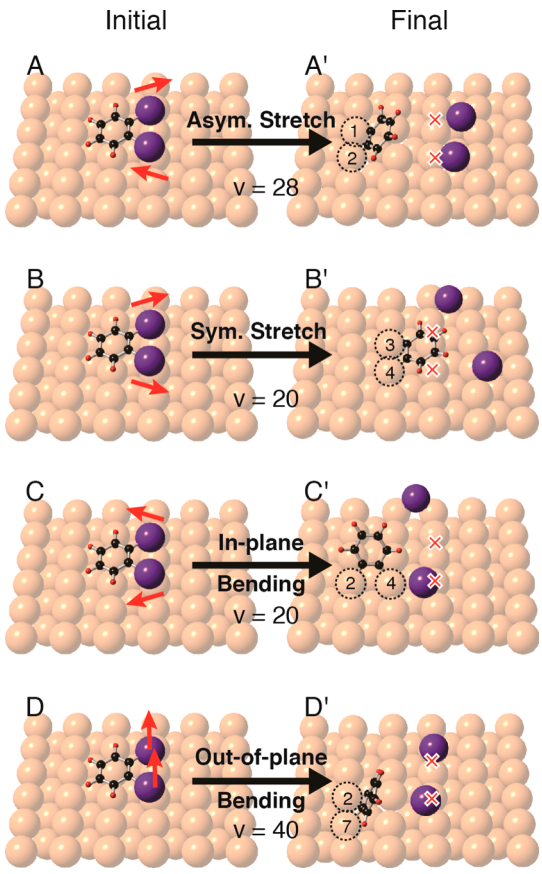

Figure 3. Left column gives four normal modes of vibration for the physisorbed *ortho*-DIB on Cu(110) involving C—I distortion: (A) asymmetric stretch of C—I bonds; (B) symmetric stretch of C—I bonds; (C) bending of C—I bonds in a plane parallel to the substrate; (D) bending of C—I bonds in a plane perpendicular to the substrate. The right-hand column (A′ to D′) gives the corresponding pattern of chemisorbed products from the lowest reactive quantum level (ν as indicated) of each normal mode that was found computationally to give product pattern at the end of each trajectory ($t = \sim 2$ ps). In the right column, the red crosses mark the prior position of I atoms in the physisorbed *ortho*-DIB (pictured at the left). The Cu atoms to which the phenylene binds are circled and numbered, following the positions labeled in Figure 1. In panel D′, #7 designates the nearest Cu atom to Cu #2 at the same Cu row but at the other side of Cu #1.

electron, it is unlikely that reaction ensues from four successive vibrational ladder-climbing events yielding such a high quantum level as $\nu = 36$ of the asymmetric stretch. As Pascual *et al.*[12] have pointed out in a pioneering study of the effect of high vibrational energy in giving migration of NH_3 across Cu(100) induced by electron-impact excitation, the path to high vibrational energy is likely to be through vibration-to-vibration (V—V) energy transfer subsequent to the excitation of a vibrational mode in resonance with the incoming electron energy. In ref 12, the authors initially excited one quantum of N—H stretch in NH_3 on Cu(100), following which intersystem crossing yielded $\nu > 30$ in a low-frequency rocking mode. In the present case, a near-resonance exists with the *ortho*-DIB C—H stretch computed here to be 0.38 eV at the copper surface.

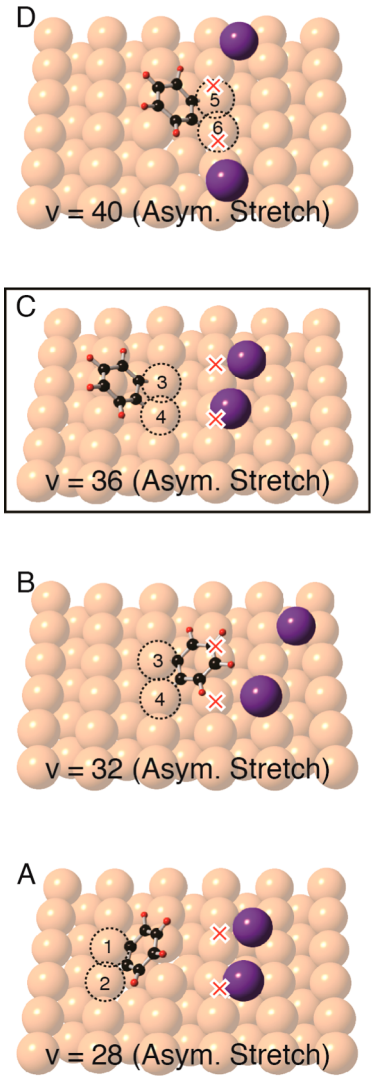

Figure 4. Patterns of chemisorbed products from different quantum levels of the asymmetric stretch mode: (A) at threshold vibrational-energy level, $\nu = 28$; (B) $\nu = 32$; (C) $\nu = 36$; (D) $\nu = 40$. The red crosses in each panel mark the position of I atoms in the physisorbed *ortho*-DIB; the Cu atoms to which the phenylene binds are circled and numbered (cf. Figure 1). (D) Cu atoms that bind the phenylene, designated 5 and 6, are located adjacent to the initial position of the I atoms. (C) is boxed to indicate that this mode of vibration leads to the observed product binding configuration in phenylene and the I atoms.

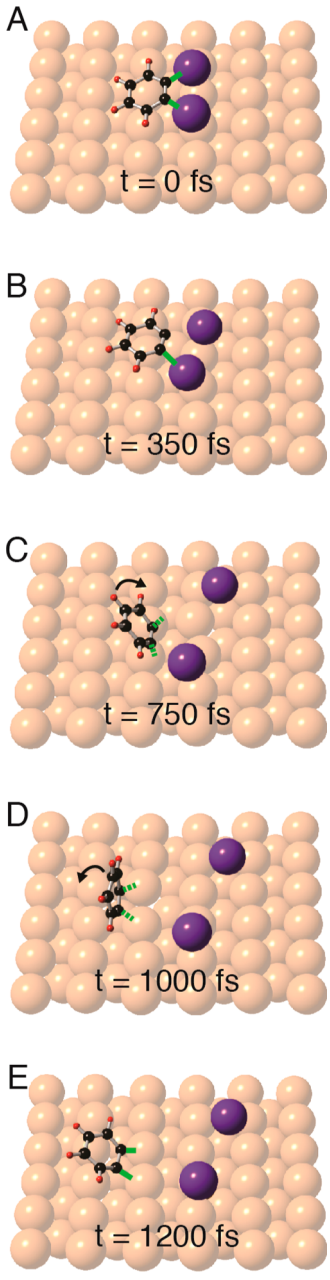

Figure 5. Reactive trajectory originating in $\nu = 36$ of the reagent asymmetric stretch mode: (A) At $t = 0$ fs, intact *ortho*-DIB (both C–I bonds marked in green) is in its most stable physisorbed configuration on Cu(110). After ~350 fs, the first C–I bond had broken, releasing the I atom at the upper part of panel B. From $t = 350$ to $t = 1000$ fs, the phenylene (Ph′) formed following the second C–I bond breaking underwent a clockwise rotation in the plane perpendicular to the Cu(110) surface, with the carbon dangling bonds attaching to the surface (C), leading to a vertical alignment of Ph′ at a four-fold hollow site, shown in (D). From $t = 1000$ to $t = 1200$ fs, Ph′ rotated counterclockwise out-of-plane to bind at the same side as the I atoms (E).

This energy level might be broadened by interaction with the surface.[34] Additionally, there exist breathing modes of the aromatic ring at 162–182 meV that could act as intermediary vibrational levels. In other laboratories, the specific pathway for vibrational excitation has been determined by the application of action spectroscopy,[25,26,35–38] which is, however, beyond the scope of the present study.

CONCLUSIONS

Scanning tunneling microscopy has been used to characterize the physisorbed initial and chemisorbed final states in the reaction of *ortho*-diiodobenzene at Cu(110), induced by inelastic collisions with electrons of 0.3 eV. This 0.3 eV excitation energy is well below the threshold of 1.0 eV reported in previous work in which reaction was ascribed to excitation to the lowest-lying electronically excited state of the physisorbed

ortho-DIB. For the present low-energy excitation, the dependence of rate on current was found to be fourth-order, and the electron efficiency was 6 to 7 orders of magnitude less than that previously found for electronic excitation of *ortho*-DIB on the same surface. We ascribe this low-electron-energy pathway to reaction induced by four successive steps of reagent vibrational excitation. The major chemisorbed products obtained by vibrational excitation exhibited a different pattern as compared to that obtained by electronic excitation. Specifically, for vibration-induced reaction, the phenylene product was shifted laterally by one lattice constant as compared with reaction by electronic excitation, and the phenylene was bound to the underlying copper by C−Cu bonds at the same side as the ejected I atoms, rather than at the opposite side as found *via* electronic excitation.

We give a simple model of the vibration-induced reaction, based on the solution of the classical equations of motion across the same *ab initio* potential-energy ground state as used in our earlier two-state model for *ortho*-DIB.[22] This time, the reaction proceeds exclusively on the ground potential-energy surface (PES), instead of both on a ground and excited PES as previously. For simplicity, we assume only single-mode vibrational excitation. The mode used corresponded to an asymmetric stretch, one of four normal modes examined, which led, when highly excited, to the binding pattern of products observed in the present experiments.

MATERIALS AND METHODS

Experiment. All experiments were performed in a low-temperature ultrahigh vacuum STM (Omicron), with a base pressure of $<3.0 \times 10^{-11}$ mbar. STM images were recorded in constant current mode at 4.6 K. The Cu(110) substrate was cleaned by repeated cycles of Ar^+ bombardment (0.6 keV, 7 μA, $P_{Ar} = 1\times 10^{-5}$ mbar, 10 min) followed by annealing (800 K, 45 min), until no contamination was detected by STM. *ortho*-Diiodobenzene (Sigma-Aldrich, 99%) was purified by several freeze−pump−thaw cycles before use in the experiment and was dosed from a capillary tube directed at the copper crystal. The crystal reached a maximum temperature of 8.3 K during dosing. Dissociation of *ortho*-DIB was electron-induced by placing the STM tip over the center of the *ortho*-DIB feature and maintaining a constant bias voltage, ±300 mV, with the feedback loop disabled, for up to ∼4 min. Prior to the bond-breaking event, the fluctuation in the current was less than 20%. Product positions with respect to the position of the physisorbed reagent were measured using WSxM.[39]

Theory. Plane-wave-based density functional theory (DFT) calculations were performed using the Vienna *ab initio* simulation package (VASP 5.2),[40,41] installed at the SciNet supercomputer.[42] The parametrizations of geometry and MD calculations are identical to our earlier work,[22,43−46] using the general gradient approximation with the Perdew−Burke−Ernzerhof functional[47] and the projector-augmented wave scheme.[48,49] The Cu(110) surface was represented by a (6 × 6) supercell that consisted of 180 Cu atoms in five layers and a vacuum gap of ∼15 Å. The surface Brillouin zone was sampled at the gamma point only. Grimme's semiempirical method (DFT-D2)[50] was employed to account for the dispersion forces in this system. The STM image simulations were generated by bSKAN.[51] Climbing image nudged elastic band method[30] was used to map the minimum-energy pathways and locate the transition states of the dissociation of *ortho*-DIB on Cu(110) for both pathways on the ground potential-energy surface. In all the calculations above, all atoms were allowed to relax except for the two bottom layers of the Cu slab until the residual force at each atom was below 0.01 eV/Å.

We also evaluated the normal modes of vibration for both initial physisorbed state and transition state following ref 52. Simply put, this method assumes a harmonic oscillator behavior and builds up a Hessian matrix using the second derivative of total energy with respect to a small displacement for each atom. Then the Hessian matrix is diagonalized to yield an eigenvector matrix and an eigenvalues matrix, from which atomic displacements and frequencies for each normal mode are extracted. In this calculation, we displaced the molecular atoms and the four Cu atoms beneath by 0.001 Å along *x*, *y*, and *z* axes while fixing all other atoms.

The DFT-MD calculations were performed by solving the equations of motion while preserving the number of atoms (N), the volume of the system (V), and the total energy (E). Conservation of total energy was obtained using a time step of 0.5 fs, which gave an average drift of total energy of less than 0.01 eV ps^{-1}. The starting geometry in each trajectory, which represented a vibrational excited state (quantum number is (v), was simply the initial physisorbed state; the definition of initial velocities of each atom was not straightforward, as given below. First, the relative displacement magnitude of each atom at certain normal mode was evaluated from the eigenvector matrix of our normal mode calculations. Second, we calculated the total vibrational energy at a level, v, as $E(v) = (v + 1/2)h\nu$, using the harmonic oscillator approximation. Third, the total vibrational energy obtained in the second step was distributed into the kinetic energy of each atom E_k, according to the mass and displacement of each atom. Fourth, the magnitude of each velocity was taken as $(2E_k/m)^{1/2}$, and the direction was simply the same as the eigenvector.

For each normal mode, we first started a trajectory from the vibrational energy equivalent to a low quantum level, $E(v) = (1/2 + v)h\nu$. Each trajectory simulation was calculated up to ∼2 ps. If no sign of reaction was observed by the end of ∼2 ps, we moved to a higher vibrational energy equivalent to the next quantum level, $E(v + 1) = (1/2 + v + 1)h\nu$, and started a new trajectory for ∼2 ps. This procedure was repeated until a reactive trajectory was obtained.

Conflict of Interest: The authors declare no competing financial interest.

Acknowledgment. We are grateful for financial support from the Natural Sciences and Engineering Research Council of Canada (NSERC) and the Xerox Research Centre Canada (XRCC). Computations were performed on the Tightly Coupled System (TCS) supercomputer at the SciNet HPC Consortium. SciNet is funded by the Canada Foundation for Innovation under the auspices of Compute Canada, the Government of Ontario, Ontario Research Fund—Research Excellence, and the University of Toronto. K.H. thanks Prof. G. Henkelman for helpful discussions at http://theory.cm.utexas.edu/forum/.

REFERENCES AND NOTES

1. Dujardin, G.; Walkup, R. E.; Avouris, Ph. Dissociation of Individual Molecules with Electrons from the Tip of a Scanning Tunneling Microscope. *Science* **1992**, *255*, 1232–1235.
2. Lu, P. H.; Polanyi, J. C.; Roger, D. Electron-Induced "Localized Atomic Reaction" (LAR): Chlorobenzene Adsorbed on Si(111)-7×7. *J. Chem. Phys.* **1999**, *111*, 9905–9907.

3. Alai, S.; Rousseau, R.; Patisas, S. N.; Lopinski, G. P.; Wolkow, R. A.; Seideman, T. Inducing Desorption of Organic Molecules with a Scanning Tunneling Microscope: Theory and Experiments. *Phys. Rev. Lett.* **2000**, *85*, 5372.
4. Sloan, P. A.; Palmer, R. E. Two-Electron Dissociation of Single Molecules by Atomic Manipulation at Room Temperature. *Nature* **2005**, *434*, 367–371.
5. Lastapis, M.; Martin, M.; Riedel, D.; Hellner, L.; Comtet, G.; Dujardin, G. Picometer-Scale Electronic Control of Molecular Dynamics Inside a Single Molecule. *Science* **2005**, *308*, 1000–1003.
6. Mayne, A. J.; Dujardin, G.; Comtet, G.; Riedel, D. Electronic Control of Single-Molecular Dynamics. *Chem. Rev.* **2006**, *106*, 4355–4378, and references therein.
7. Yoder, N. L.; Guisinger, N. P.; Hersam, M. C.; Jorn, R.; Kaun, C.- C.; Seideman, T. Quantifying Desorption of Saturated Hydrocarbons from Silicon with Quantum Calculations and Scanning Tunneling Microscopy. *Phys. Rev. Lett.* **2006**, *97*, 187601.
8. Hla, S. W.; Meyer, G.; Rieder, K.-H. Inducing Single-Molecule Chemical Reactions with a UHV-STM: A New Dimension for Nano-Science and Technology. *Chem. Phys. Chem.* **2001**, *2*, 361–366, and references therein.
9. Sakulsermsuk, S.; Sloan, P. A.; Palmer, R. E. A New Mechanism of Atomic Manipulation: Bond-Selective Molecular Dissociation *via* Thermally Activated Electron Attachment. *ACS Nano* **2010**, *4*, 7344–7348.
10. Huang, K.; McNab, I. R.; Polanyi, J. C.; Yang, J. (S. Y.) Adsorbate Alignment in Surface Halogenation: Standing up Is Better than Lying Down. *Angew. Chem., Int. Ed* **2012**, *51*, 9061–9065.
11. Hla, S. W.; Bartels, L.; Meyer, G.; Rieder, K.-H. Inducing All Steps of a Chemical Reaction with the Scanning Tunneling Microscope Tip: Towards Single Molecule Engineering. *Phys. Rev. Lett.* **2000**, *85*, 2777–2780.
12. Pascual, J. I.; Lorente, N.; Song, Z.; Conrad, H.; Rust, H. P. Selectivity in Vibrationally Mediated Single-Molecule Chemistry. *Nature* **2003**, *423*, 525–528.
13. Komeda, T.; Kim, Y.; Kawai, M.; Persson, B. N. J.; Ueba, H. Lateral Hopping of Molecules Induced by Excitation of Internal Vibration Mode. *Science* **2002**, *295*, 2055–2058.
14. Ho, W. Single-Molecule Chemistry. *J. Chem. Phys.* **2002**, *117*, 11033–11061, and references therein.
15. Maksymovychi, P.; Sorescu, S. D.; Jordan, K. D.; Yates, J. T., Jr. Collective Reactivity of Molecular Chains Self-Assembled on a Surface. *Science* **2008**, *322*, 1664–1667.
16. Leung, L.; Lim, T.; Polanyi, J. C.; Hofer, W. A. Molecular Calipers Control Atomic Separation at a Metal Surface. *Nano Lett.* **2011**, *11*, 4113–4117.
17. Morgenstern, K.; Lorente, N.; Rieder, K.-H. Controlled Manipulation of Single Atoms and Small Molecules Using the Scanning Tunneling Microscope. *Phys. Status Solidi B* **2013**, *250*, 1671–1751, and references therein.
18. Cheng, F.; Ji, W.; Leung, L.; Ning, Z.; Polanyi, J. C.; Wang, C.-G. How Adsorbate Alignment Leads to Selective Reaction. *ACS Nano* **2014**, *8*, 8669–8675.
19. Shen, T. C.; Wang, C.; Abeln, G. C.; Tucker, J. R.; Lyding, J. W.; Avouris, Ph.; Walkup, R. E. Atomic Scale Desorption through Electronic and Vibrational Excitation Mechanisms. *Science* **1995**, *268*, 1590–1592.
20. Shi, H.-J.; Jung, J.; Motobayashi, K.; Yanagisawa, S.; Morikawa, Y.; Kim, Y.; Kawai, M. State-Selective Dissociation of a Single Water Molecule on an Ultrathin MgO Film. *Nat. Mater.* **2010**, *9*, 442–447.
21. Soukiassian, L.; Mayne, A. J.; Carbone, M.; Dujardin, G. Atomic-Scale Desorption of H Atoms from the Si(100)−2 × 1:H Surface: Inelastic Electron Interactions. *Phys. Rev. B* **2003**, *68*, 035303.
22. Huang, K.; Leung, L.; Lim, T.; Ning, Z.; Polanyi, J. C. Single-Electron Induces Double-Reaction by Charge Delocalization. *J. Am. Chem. Soc.* **2013**, *135*, 6220–6225.
23. Chatterjee, A.; Cheng, F.; Leung, L.; Luo, M.; Ning, Z.; Polanyi, J. C. Molecular Dynamics of the Electron-Induced Reaction of Diiodomethane on Cu(110). *J. Phys. Chem. C* **2014**, *118*, 25525–25533.
24. Electronic excitation (321 cases) gave two minor outcomes: one (16%) with Ph′ bound to two Cu atoms adjacent to the two I atoms and the other with Ph′ vertical (17%). Vibrational excitation (61 cases) also gave two minor pathways: one (16%) with Ph′ bound at a distance from the two I atoms and the other with Ph′ vertical (20%).
25. Huang, T.; Zhao, J.; Feng, M.; Popov, A. A.; Yang, S.; Dunsch, L.; Petek, H. A Molecular Switch Based on Current-Driven Rotation of an Encapsulated Cluster within a Fullerene Cage. *Nano Lett.* **2011**, *11*, 5327–5332.
26. Motobayashi, K.; Kim, Y.; Arafune, R.; Ohara, M.; Ueba, H.; Kawai, M. Dissociation Pathways of a Single Dimethyl Disulfide on Cu(111): Reaction Induced by Simultaneous Excitation of Two Vibrational Modes. *J. Chem. Phys.* **2014**, *140*, 194705.
27. Krishna, V.; Tully, J. C. Vibrational Lifetimes of Molecular Adsorbates on Metal Surfaces. *J. Chem. Phys.* **2006**, *125*, 054706.
28. Bartels, L.; Meyer, G.; Rieder, K. H.; Velic, D.; Knoesel, E.; Hotzel, A.; Wolf, M.; Ertl, G. Dynamics of Electron-Induced Manipulation of Individual CO Molecules on Cu(111). *Phys. Rev. Lett.* **1998**, *80*, 2004–2007.
29. There is a computed barrier of 0.34 eV from final state ELEC to VIB, by climbing image nudged elastic band calculations.
30. Henkelman, G.; Uberuaga, B. P.; Jonsson, H. A Climbing Image Nudged Elastic Band Method for Finding Saddle Points and Minimum Energy Paths. *J. Chem. Phys.* **2000**, *113*, 9901.
31. Varsanyi, G.; Kovner, M. A.; Lang, L. *Assignment for Vibrational Spectra of Seven Hundred Benzene Derivatives*; Wiley: New York, 1974; p 261.
32. The two bending modes also involve a small deformation of the aromatic ring.
33. The trajectory originating at the threshold of $\nu = 28$ of the asymmetric stretch gave a product distribution corresponding to a minor (16%) pathway observed in the experiments with reagent vibrational excitation.
34. Han, P.; Weiss, P. S. Electronic Substrate-Mediated Interactions. *Surf. Sci. Rep.* **2012**, *67*, 19–81.
35. Sainoo, Y.; Kim, Y.; Okawa, T.; Komeda, T.; Shigekawa, H.; Kawai, M. Molecular Vibrational Modes with Inelastic Scanning Tunneling Microscopy Processes: Examination through Action Spectra of *cis*-2-Butene on Pd(110). *Phys. Rev. Lett.* **2005**, *95*, 246102.
36. Parschau, M.; Passerone, D.; Rieder, K.-H.; Jug, H. J.; Ernst, K.-H. Switching the Chirality of Single Adsorbate Complexes. *Angew. Chem., Int. Ed.* **2009**, *48*, 4065–4068.
37. Motobayashi, K.; Kim, Y.; Ueba, H.; Kawai, M. Insight into Action Spectroscopy for Single Molecule Motion and Reactions through Inelastic Electron Tunneling. *Phys. Rev. Lett.* **2010**, *105*, 076101.
38. Frederiksen, T.; Paulsson, M.; Ueba, H. Theory of Action Spectroscopy for Single Molecule Reactions Induced by Vibrational Excitation with STM. *Phys. Rev. B* **2014**, *89*, 035427.
39. Horcas, I.; Fernández, R.; Gómez-Rodríguez, J. M.; Colchero, J.; Gómez-Herrero, J.; Baro, A. M. WSXM: A Software for Scanning Probe Microscopy and a Tool for Nanotechnology. *Rev. Sci. Instrum.* **2007**, *78*, 013705.
40. Kresse, G.; Hafner, J. *Ab Initio* Molecular Dynamics for Liquid Metals. *Phys. Rev. B* **1993**, *47*, 558.
41. Kresse, G.; Furthmüller, J. Efficient Iterative Schemes for *Ab Initio* Total-Energy Calculations Using a Plane-Wave Basis Set. *Phys. Rev. B* **1996**, *54*, 11169–1118.
42. Loken, C.; Gruner, D.; Groer, L.; Peltier, R.; Bunn, N.; Craig, M.; Henriques, T.; Dempsey, J.; Yu, C.-H.; Chen, J.; Dursi, L. J.; Chong, J.; Northrup, S.; Pinto, J.; Knecht, N.; Van Zon, R. SciNet: Lessons Learned from Building a Power-Efficient Top-20 System and Data Centre. *J. Phys.: Conf. Ser.* **2010**, *256*, 012026.
43. Eisenstein, A.; Leung, L.; Lim, T.; Ning, Z.; Polanyi, J. C. Reaction Dynamics at a Metal Surface; Halogenation of Cu(110). *Faraday Discuss.* **2012**, *157*, 337–353.
44. Leung, L.; Lim, T.; Ning, Z.; Polanyi, J. C. Localized Reaction at a Smooth Metal Surface: *p*-Diiodobenzene at Cu(110). *J. Am. Chem. Soc.* **2012**, *134*, 9320–9326.

45. Ning, Z.; Polanyi, J. C. Charge Delocalization Induces Reaction in Molecular Chains at a Surface. *Angew. Chem., Int. Ed.* **2013**, *52*, 320–324.
46. Ning, Z.; Polanyi, J. C. Catalyzed Surface-Aligned Reaction, H(ad) + H_2(ad) = H_2(g) + H(ad) on Coinage Metals. *Z. Phys. Chem.* **2013**, *227*, 1–10.
47. Perdew, J. P.; Ernzerhof, M.; Burke, K. Rationale for Mixing Exact Exchange with Density Functional Approximations. *J. Chem. Phys.* **1996**, *105*, 9982.
48. Blochl, P. E. Projector Augmented-Wave Method. *Phys. Rev. B* **1994**, *50*, 17953.
49. Kresse, G.; Joubert, D. From Ultrasoft Pseudopotentials to the Projector Augmented-Wave Method. *Phys. Rev. B* **1999**, *59*, 1758.
50. Grimme, S. Semiempirical GGA-Type Density Functional Constructed with a Long-Range Dispersion Correction. *J. Comput. Chem.* **2006**, *27*, 1787.
51. Palotás, K.; Hofer, W. A. Multiple Scattering in a Vacuum Barrier Obtained from Real-Space Wavefunctions. *J. Phys.: Condens. Matter* **2005**, *17*, 2705–2713.
52. Henkelman, G.; Arnaldsson, A.; Jonsson, H. Theoretical Calculations of CH_4 and H_2 Associative Desorption from Ni(111): Could Subsurface Hydrogen Play an Important Role? *J. Chem. Phys.* **2006**, *124*, 044706.